epithelium and CA [2]. These facts imply that there are sequential stages of ADs, ranging from almost normal (i.e., hyperplastic polyp) to nearly cancerous forms. The ability to identify high-risk ADs and to predict the likelihood of a lesion becoming malignant would be very useful clinically.

For the accurate diagnosis of colorectal cancer, it is important to identify a gene set that is useful as marker of neoplasia. Although alterations in the genomic structure of the K-ras oncogene and the tumor suppressor genes APC, DCC, and p53 have been reported to be strongly involved in colorectal carcinogenesis [3–6], no gene set whose aberrant expression perfectly corresponds with the pathologic stage of every colorectal malignancy has yet been identified. To avoid misdiagnosis by chance because of statistical fluctuation resulting from a small number of genes, the use of at least 10 genes in the multigene expression signature is recommended, and DNA microarray technology is suitable for generating this signature [7]. To accommodate large sets of expression data, several methods have been developed to classify two distinct states (or classes), such as tumors versus clinically normal samples or subtypes with different prognoses, in light of genes differentially expressed between the two classes [7–9]. The appropriateness of the classification from these methods relies much on the samples used as a "training set," because of fundamental characteristics of the methods. Therefore, we tried to develop a method of selecting genes that would be less dependent on the training set used and that would have more potential to predict latent malignancy. In addition, the candidate gene set used as a predictor of malignancy must assign the CA state with 100% sensitivity, because misclassifying benign lesions as malignant (i.e., false-positive classification) likely would be more preferable than misclassifying malignant lesions as benign (i.e., false-negative classification) in clinical diagnosis [9,10]. We focused on selecting genes to create a predictor set that (1) was 100% sensitive for predicting malignant samples as malignant and (2) had the potential for predicting latent malignancy. We call our method the ADMS and describe its strategy in detail later. By applying our ADMS (algorithm for diagnosing malignant state) method to the gene expression data derived from seven ADs and 16 CAs, we successfully selected 335 clones characteristic of the malignant state of colorectal CAs. We, then, successfully used this clone set to characterize 12 additional tumors including primary tumors with metastasis and metastatic tumors.

Materials and methods

Patients and samples. We obtained 35 operative specimens (including 21 primary colorectal carcinomas, seven colorectal adenomas, five liver metastases, and two lung metastases) from 24 patients. None of the patients with adenoma or primary colorectal cancer had received any other therapy previously. Our patient population comprised 17 patients (age, 38–77 years) with well- ($n = 10$) or moderately- ($n = 7$) differentiated adenocarcinoma and seven patients (age, 39–87 years) with mild ($n = 1$) or moderate ($n = 5$) dysplasia or serrated adenoma ($n = 1$) of the colorectum who underwent resection at Yokohama City University in Japan (Table 1). Samples (including normal colonic mucosa) were frozen in liquid nitrogen as soon as possible in the surgery suites and stored at −80 °C before use.

Table 1
Summary of characteristics in various colorectal specimens

Sample	R^a	Tumor size (mm)
Adenoma		
AD1	0.775927	7
AD2	0.791106	15
AD3	0.793689	5
AD4	0.77645	12
AD5	0.715965	25
AD6	0.584908	25
AD7	0.791039	10
Carcinoma		
CA1	0.931021	10
CA2	0.753601	20
CA3	0.845746	90
CA4	0.86255	15
CA5	0.868843	65
CA6	0.803393	38
CA7	0.803198	70
CA8	0.713931	26
CA9	0.669531	90
CA10	0.580932	34
CA11	0.925502	55
CA12	0.819892	70
CA13	0.831103	50
CA14	0.652069	45
CA15	0.715589	60
CA16	0.687025	25
meta_pri1	0.72009	
meta_pri2	0.889506	
meta_pri3	0.837234	
meta_pri4	0.918368	
meta_pri5	0.888062	
Metastatic lesion		
meta_liver1	0.818897	
meta_liver2	0.681267	
meta_liver3	0.761274	
meta_liver4	–	
meta_liver5	0.845192	
meta_lung1	0.637546	
meta_lung2	0.882046	

Samples AD1–7, CA1–16, and meta_pri1-5 were obtained from primary colorectal tumors. Tumors CA11–16 and meta_pri1-5 were metastatic to lymph nodes by histology. In addition, the tumors for the meta_pri1–5 samples caused hepatic metastasis; samples meta_liver1–5 derived from these liver metastases. Samples meta_lung1 and 2 were from lung metastases. The data from AD1–7 and CA1–16 were used as a "training set" for identifying genes characteristic of the malignant (CA) state, and the remaining samples were used as an independent set to test our method.

[a] Correlation coefficient of the expression ratio in the duplicate experiment after PRIM filtration. The meta_liver4 sample lacks this information because of the failure of an experiment.

Human 21K array. The target DNAs used to construct human 21K array were the glycerol stock cDNA clones purchased from Research Genetics (http://www.resgen.com/). Total of 20,784 clones with positive and negative controls were printed. After plasmid DNAs were extracted, the PCR amplification using universal primers was performed. The PCR products were, then, precipitated with isopropyl alcohol and resuspended in 15 μl of 3× SSC. The DNA solution was spotted on poly (L-lysine)-coated slides by using RIKEN DNA arrayer with 48 tips (SMP3, TeleChem International, Sunnyvale, CA). The detailed protocol was described elsewhere [11].

RNA extraction. We homogenized 2 g of each sample in 20 ml solution D, then added 2 ml 2 M sodium acetate, 16 ml water-saturated phenol, and 4 ml chloroform and mixed vigorously. After storage on ice for 15 min, samples were centrifuged (6000*g*, 30 min, 4 °C). The aqueous layer was carefully aspirated and added to 20 ml isopropanol and stored overnight in −20 °C. Afterwards, the solution was centrifuged (7500*g*, 15 min, 4 °C), and the resulting RNA pellet was washed with 75% ethanol and centrifuged (7500*g*, 5 min, 4 °C). The RNA was resuspended in 4 ml RNase-free water, to which we added 1.3 ml 5 M NaCl and 16 ml CTAB/UREA. The mixture was centrifuged at 7500*g* for 15 min at room temperature. We added 4 ml 7 M guanidine–HCl and 100% ethanol to the supernatant and stored it overnight at −20 °C. The solution was then centrifuged and washed as described previously, and the RNA was resuspended in 500–1000 μl RNase-free water. The quality of the RNA was checked by electrophoresis.

Fluorescent probe, hybridization, and screening. Hundred μg of total RNA was labeled with the fluorescent dye Cy3 (cancer or adenoma tissue) or Cy5 (normal mucosa) by SuperScript II (Gibco). Three samples of normal colon mucosa were mixed to provide a reference sample. Hybridization to the human 21K array was carried out in a 65 °C water bath for 6 h. Slides then were washed in 0.1% SDS in 2× SSC for 5 min, 1× SSC for 5 min, and 0.2× SSC for 15 min at room temperature. These slides were scanned on a ScanArray5000 confocal laser scanner (Packard Inst.), and the images were analyzed by using ScanAlyze (Stanford University). Each spot was defined by manually positioning a grid of circles over the array image, and spots deemed unsuitable for accurate quantitation because array artifacts were flagged and excluded from analysis. The duplicate experiments were performed by using the same template mRNA, but the labeling and hybridization were done separately for each experiment.

Data processing. To select reproducible spots from the microarray experiments, we ran the PRIM filtration program [12] on the ScanAlyze program output files. Briefly, this data processing method extracts reproducible data efficiently from the ScanAlyze output files of duplicate experiments and outputs averaged value of $\log_2$(cy3/cy5) to the duplicate experiments. In this process, the threshold value for filtering data is optimized by using the product of N and R, where N is the ratio of the number of spots that passed the filtering to the total number of spots, and R is the correlation coefficient for the results obtained from the duplicate experiments. The average R overall was 0.7665 (SD, 0.0905). We constructed a gene expression matrix in which genes (clones) were placed in rows, and columns corresponded to the carcinogenesis classification (e.g., CA versus AD).

Results

We studied a series of colorectal specimens (total, 35 samples) by using microarray technology. All the experiments were performed in duplicate. We hybridized Cy3-labeled human cDNA probes from tumor (carcinoma or adenoma) samples to Cy5-labeled cDNA probes corresponding to normal colon mucosa. The resulting output files produced by scanning and image analysis were processed further by using the rational filtration program PRIM to pick up the reproducible data [12]. We then constructed the gene expression matrix in which each row represents one of the 20,784 clones in the array, and the columns correspond to series of samples.

Gene selection and sample classification

Using the gene expression matrix from the training set (i.e., the subset of all samples used), we used our ADMS method (Fig. 1) to select clones that satisfy the following conditions for characterizing the CA state:

$$\overline{r_{ik}^{jth}} < \overline{r_{ik}^{all}} \quad \text{and} \quad \overline{r_{ik}^{jth}} > \overline{r_{ik}^{all}}, \tag{1}$$
$$(i,k\in CA,\, i\neq k) \qquad (i\in AD,\, k\in CA)$$

where $\overline{r_{ik}}$ is the average correlation coefficient (r) between sample i and sample k, $\overline{r_{ik}^{all}}$ is $\overline{r_{ik}}$ for all clones (n) in the original set, and $\overline{r_{ik}^{jth}}$ is $\overline{r_{ik}}$ for all clones but the jth ($j = 1,2,\ldots,n$). Disregarding the effect of the compaction in AD samples, the separation between benign and malignant samples in ADs was expected.

After the predictor clones were extracted by using the training set, we calculated the classification score S for sample x as

$$S = \underset{(k\in CA)}{\overline{r_{xk}}} - \underset{(k\in AD)}{\overline{r_{xk}}}, \tag{2}$$

where $\overline{r_{xk}}$ is the average r of x against sample set k. If $S > 0$, the sample x is assigned to be in the CA state; otherwise, x is assigned to be non-CA.

We then applied ADMS to select clones characteristic of the malignant (i.e., CA) state from those represented in the clone expression matrix by using seven adenomas (AD1–7) as benign cases and 16 carcinomas (CA1–16) as malignant ones (Table 1). We used the leave-one-out cross validation (LOOCV) method on the carcinoma (CA1–16) samples to show the accuracy of ADMS. In LOOCV, the method omits a CA sample, selects candidate clones in light of the remaining samples, and evaluates whether the omitted sample is assigned to CA (Fig. 1). We limited the use of LOOCV to the CA samples because of several reasons: (1) specimens classified as AD do not always remain AD—some progress to a malignant state; (2) CA lesions practically never revert to an AD state; and (3) some of the differences in mRNA expression observed in carcinomas also will occur in the adenomas [2]. Therefore, we restricted our LOOCV analysis to using CAs to attempt to achieve a classification performance with 100% sensitivity.

The characterization of each sample as CA or non-CA by using the candidate clones derived from the LOOCV test showed that all 16 assignments coincided with the clinical diagnosis (Fig. 2). Further, the S value for each sample was higher than that for a 1% significance level, as calculated by the random selection of each number of genes with 1000 repetitions. In addition,

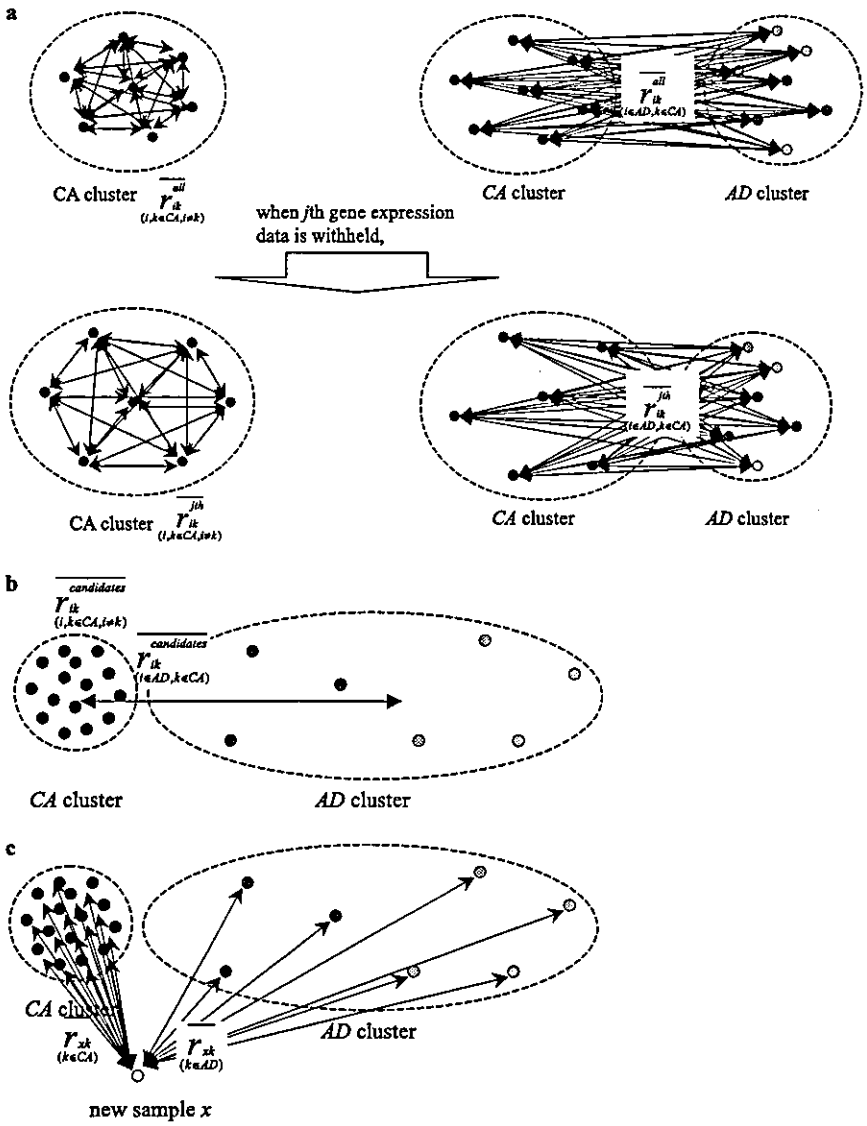

Fig. 1. Schematic diagram of the ADMS method. (a) Schematic diagram of selecting candidate genes characteristic of the carcinoma (CA) state. The candidates were selected in light of the following criteria: when the gene was withheld, the average of the Pearson correlation coefficients within CA samples across all genes ($\overline{r_{ik}^{all}}(i,k \in \mathrm{CA},\ i \neq k)$) is higher than that across all but the jth (remaining) gene ($\overline{r_{ik}^{\setminus jth}}(i,k \in \mathrm{CA},\ i \neq k)$), and the average of Pearson correlation coefficients between CA and adenoma (AD) samples across all the genes ($\overline{r_{ik}^{all}}(i \in \mathrm{AD},\ k \in \mathrm{CA})$) is lower than that across those remaining ($\overline{r_{ik}^{\setminus jth}}(i \in \mathrm{AD},\ k \in \mathrm{CA})$). (b) Expected features of genes selected by the procedure in (a). The selected candidates (especially those strongly indicative of the CA state), which frequently emerged in the leave-one-out cross-validation (LOOCV) analysis (see Results), must have high $\overline{r_{ik}^{candidates}}(i,k \in \mathrm{CA},\ i \neq k)$ and low $\overline{r_{ik}^{candidates}}(i \in \mathrm{AD},\ k \in \mathrm{CA})$. (c) Classification of the sample x, where the evaluation is based on Eq. (2) using the candidate predictor genes. Sample x is categorized as either CA or non-CA.

we observed that the LOOCV analysis returned a various number of candidate clones depending on the sample omitted. The 335 clones common to all 16 CAs included 135 known genes that were considered strong candidates for diagnosing the cancer state. The 200 clones list excluding 135 known genes is provided as a supplementary information.

The classification score S of all 35 samples (including 12 metastatic samples) as the test set was re-evaluated, in which CA consisted of CA1–16, and query sample itself was not included in set k in Eq. (2) (Fig. 3). The higher the S score, the closer the expression profile of the specimen is to that of the CA state. The classification scores of all of the metastatic and primary lesions used in the test set had higher (positive) values than those needed for a 1% significance level, whereas those of four of the seven AD samples (AD1–4) showed negative values. In contrast, samples AD5–7 had positive S scores. Of these, tumors AD5 and AD6 were larger than those with low S values (Table 1).

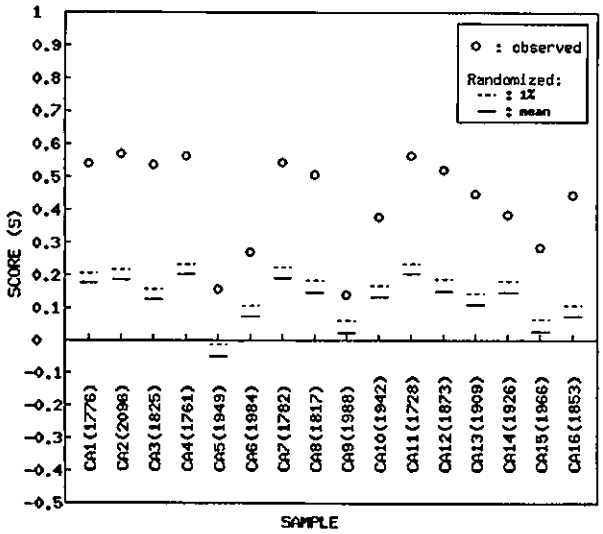

Fig. 2. Classification scores of 16 CA samples in LOOCV analysis. Each sample label designates the sample withheld in the LOOCV analysis and evaluated as the unknown sample. The number in parenthesis is the number of genes selected when the corresponding sample is withheld. Classification scores for each of sample are denoted as circles. Mean classification scores, calculated from 1000-fold iteration in which the corresponding number of genes in the sample was selected randomly, are denoted as the horizontal line above each of the samples. The 1% significance levels are denoted as the dashed lines. Note that all observed scores are higher than that of the corresponding 1% significance level.

To evaluate the effect of differences in the training set on the fluctuation level of the classification score S, we constructed 16 sub-training sets consisting of 15 CAs (a set in which the jth ($j = 1,2,\ldots,16$) sample is omitted from the original 16 CAs) and the seven ADs. Then, we evaluated each of the subtracted CAs as a test set by using the same procedure with which 335 clones were selected previously. As a result, 16 classification scores (15 from when a CA sample was included in the training set and ine from when that sample was the test set) were produced for each of the 35 samples evaluated (Fig. 4a). All of the scores for cancer (CA and metastasis-related) samples had positive values, indicating that the accuracy of ADMS is 100%. If our method was sensitive to the training set used, the score of a sample when evaluated as test set would be lower than those when the sample was included in the training sets. Although nine of the 16 CA samples had such low scores, the scores of the remaining (CA1, 3, 4, 7, 11, 14, and 16) were higher than that for the 1% significance level associated with the 15 scores obtained when a sample was included in a training set (data not shown). These findings suggest that our method is not particularly sensitive to the characteristics of the training set.

We compared results from our ADMS with those obtained by using the widely known Golub's method [7], which aims to select genes that can classify two different conditions. We adopted Golub's method to see the fluctuations and accuracy of prediction associated with using the same set described above (Fig. 4b). The Golub method selects the predictor genes from the training set by using "neighborhood analysis" and assigns unknown samples by using a "weighted-voting algorithm" [7]. The neighborhood analysis chose the same number of clones as ADMS did. With the weighted-voting algorithm, the "prediction strength (PS)" was calculated as a classification score. If PS > 0, the sample was classified as CA; otherwise, the sample was classified as AD. As a result, the PS of CA9 when evaluated as a test set was negative. That is, the weighted-voting algorithm returned a false-negative result, which would be detrimental to actual, clinical diagnosis [9]. Although the scores of the remaining cancer samples led to correct classification results, the score of each CA when evaluated as a test set (red circles in Fig. 4b) was the lowest value of the 16 scores of each CA. In addition, these test set-associated values exceeded the threshold for the 1% significance level of the 15 scores when the sample was included in the training set (data not shown). These results suggest that Golub's method has a tendency to "over fit" to the genes characterizing the CA state in the training set.

Among the 335 clones we identified as strong candidates for markers of malignancy, the expression profiles of the 135 known genes were delineated according to the cellular functions apoptosis, cell adhesion, cell cycle, signal transduction, gene expression, and miscellaneous (Fig. 5). Many of the assignments we made are consistent with those reported in the literature. The most striking example is the expression profiles of apoptosis-related genes, whose expression is down-regulated in lesions in a malignant state (including the "precancerous" AD5-7 samples) but up-regulated in the benign state, corresponding to our intuition about the multistep progression of cancer. Two-hundred clones list excluding 135 known genes (Fig. 5) is shown as a supplementary information.

Discussion

We have developed the ADMS method to extract clones that can feature the malignant characteristics using the expression profile data. ADMS was applied using 16 CA samples and seven AD samples. Three-hundred and thirty-five clones were finally selected as common ones after repeating LOOCV method.

Of the 20,784 human clones on a microarray chip, about 1900 clones were selected during each LOOCV for the CA1–16 samples (Fig. 2). All the CA lesions were correctly diagnosed as cancerous state. Our ADMS method selects malignancy marker clones by the following criteria: (1) the average Pearson correlation coefficient (r) of expression profiles among all the combinations of clones within CA samples but the clone

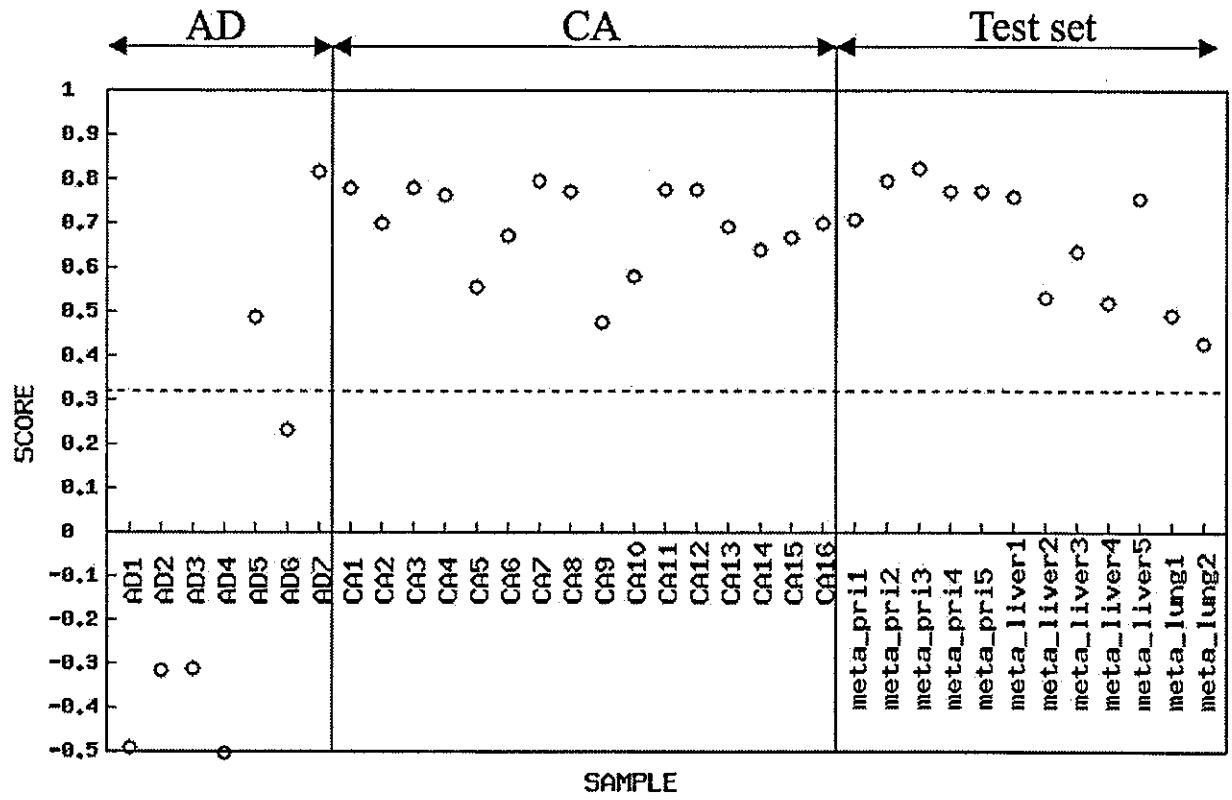

Fig. 3. Classification scores of all 35 samples by using the 335-gene predictor set. All samples including the 12-sample test set were evaluated. The 1% significance level (dashed line) was calculated from 16,000 data points: (1) 335 genes were selected randomly, (2) the classification score of each of the 16 CA samples was calculated, (3) this process was iterated 1000 times. All scores of cancer samples showed were positive values, which also were higher than that of the 1% significance level (100% sensitivity). In addition, two of three adenomas that had positive scores were relatively large (≥25 mm) and were larger than the four adenomas with negative scores. This result suggests that ADMS has the potential of screening for high-risk adenomas.

of interest is lower than that among all the combinations within CA samples, and (2) the average r of the expression profiles among all combinations of clones in the CA and AD samples but the clone of interest is higher than that among all the combinations of CA and AD samples. We expected the rational separation between benign and malignant samples in AD samples by not regarding the additional criteria of AD samples in the above criteria (1) about CA samples.

The governing idea of our method arises from several facts and ideas. First, AD occupies a biological position between normal colon epithelium and CA, and the abnormalities in mRNA expression observed in carcinomas also may be present in the ADs [2]. ADs can range in nature from a completely benign state to nearly cancerous. Means of identifying AD samples or states with a strong potential for malignant conversion likely will be useful for effective diagnosis and therapy. Second, false-negative errors (tumor samples being classified as normal) can be detrimental, whereas false-positive results (normal samples being classified as tumor) are more easily tolerated clinically [9,10]. This idea is applicable to the assignment of CA (malignant) versus AD (benign) classifications. Accordingly, we aimed at 100% accuracy in diagnosing CA samples and have been screening additional latently malignant AD samples by using our ADMS universal evaluation system.

We demonstrated the feasibility of our ADMS method by using classification scores ($S > 0$) and by $S > 1\%$ significance level, produced by 1000-fold iteration of random clone selection test. All scores of CAs in LOOCV were higher than 0 with 1% significance level. However, the number of clones selected by an LOOCV analysis ranged from 1728 to 2096, depending on the test sample. As our predictor set we chose the 335 clones that were common to all 16 test cases. We assumed this set was a very robust one featuring the malignant state, and further evaluated the feasibility of this set using another sample set including five primary colon cancer with metastatic lesion and seven metastatic tumors.

Using the 335-clone predictor set classified 31 (16 CAs, 12 test samples, and three ADs) samples as CA and the remaining four as non-CA (Fig. 3). Of the 31 CA classifications, those for all 28 malignant samples (16 CAs and 12 test samples) coincided with the clinical diagnosis

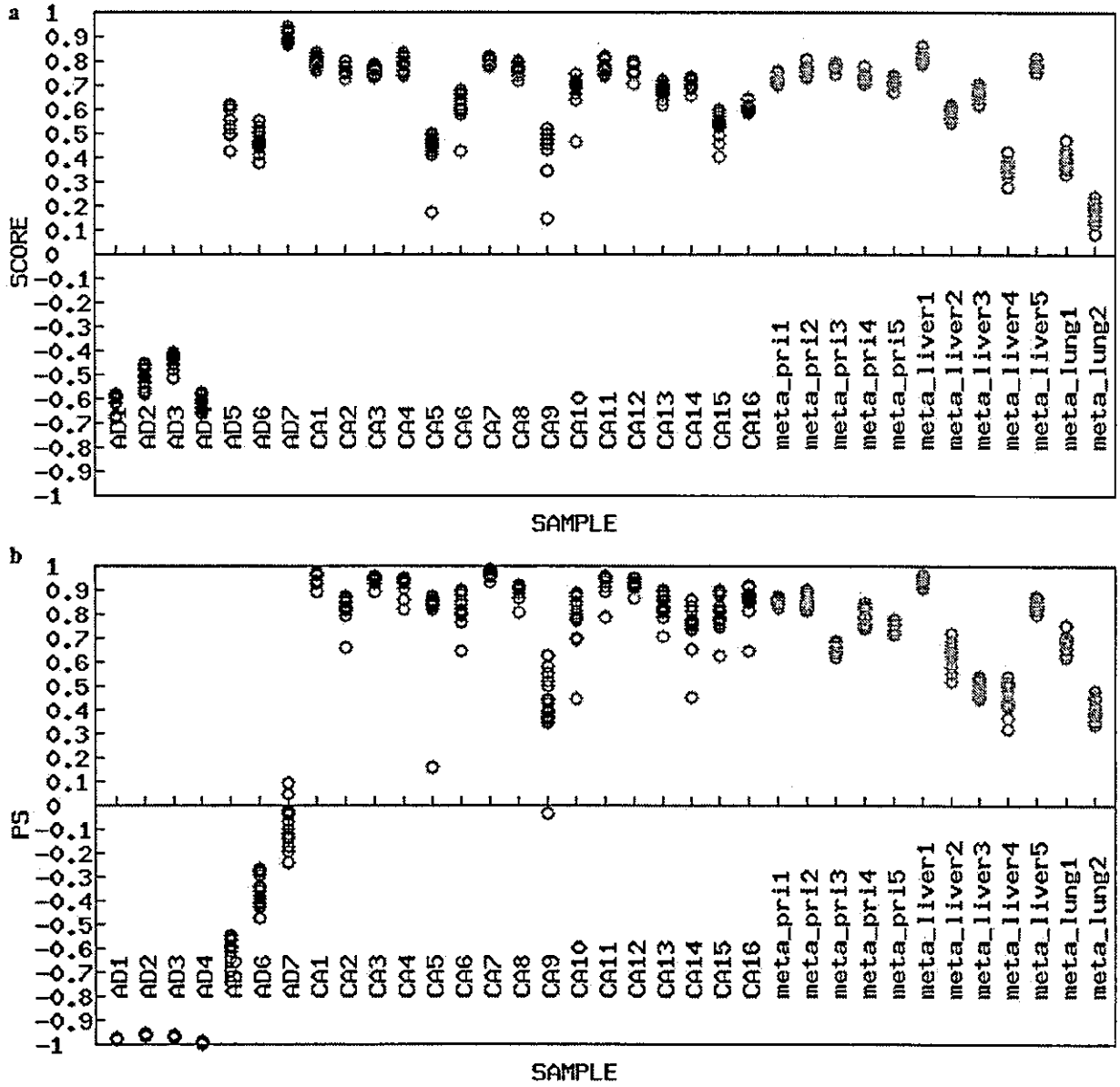

Fig. 4. Fluctuation in classification scores upon changing the training set. For each sample, the black circles correspond to the 15 scores obtained when the sample is included in the training set; the red circle denotes the score when the designated sample is the test sample. (a) Results from the ADMS method. (b) Results from Golub's method. Positive value for both scores shows assignment to CA states. Unlike Golub's, our method shows 100% sensitivity ($S > 0$) for cancer classification (CA and metastatic). Note also that ADMS is less sensitive to changes of the training set than is Golub's method.

(100% sensitivity). Two (AD5 and AD6) of the three AD samples had relatively large tumor size (>25 mm; see Table 1). This result is reasonable, because tumor size is one of the indicators for potential malignancies. However, AD7 lacked any such characteristic suggestive of cancer, thus suggesting a false-positive error. This result might have been caused because we have not included the criteria for true-negative classification (AD samples being classified as AD) in our method. Further follow-up of this patient should clarify this argument.

In the 12 test samples, the classification scores of "meta_pri1-5" were similar to those of the CA samples, whereas the other seven metastatic samples were relatively lower in score than were the primary lesions (see Fig. 3). These findings suggest that this tendency may reflect the heterogeneity of the sample tissues. Nonetheless, this result showed that we can diagnose malignancy in light of the expression profile of the tumor samples without using laser capture microdissection [13] because of the high classification

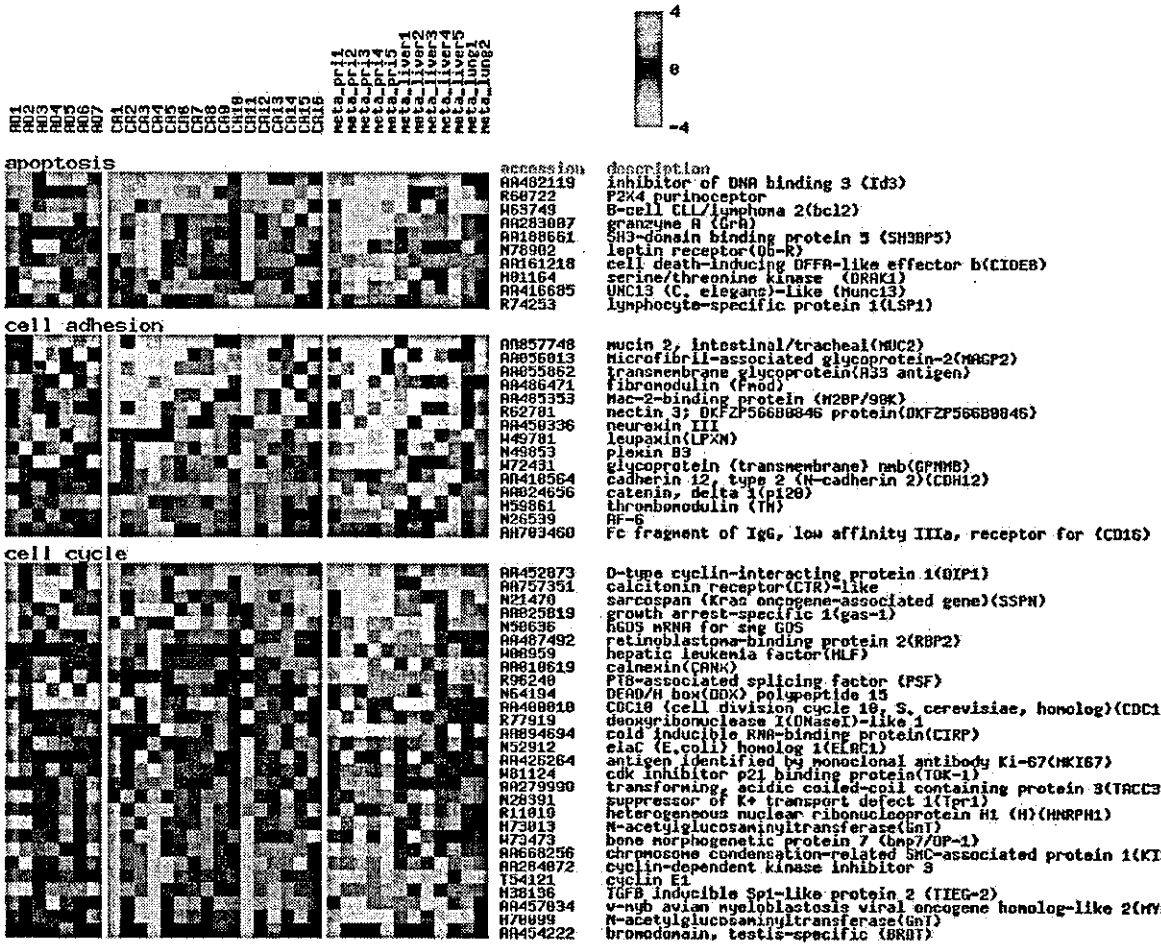

Fig. 5. The 135 known genes among the 335 candidates strongly predictive of the CA state. Each row corresponds to a gene, and the columns correspond to its expression levels in different samples. The genes are allocated according to the cellular functions apoptosis, cell adhesion, cell cycle, signal transduction, gene expression, and miscellaneous. Gene expression ratios are depicted according to the color scale shown at the top right. Gray indicates missing or excluded data. The expression profiles of many of these genes were consistent with those reported in the literature.

scores of those samples with statistical significance ($P < 0.01$).

Although many methods have been developed for identifying genes that discriminate two different conditions by using the expression profile, the utility of most of them is heavily dependent on nature of the training set. Development of a method that is relatively insensitive to variability in the training set is essential to avoid misdiagnosis, and ADMS was less sensitive to this type of variability than was Golub's method (Fig. 4). Further, our results revealed a 100% sensitivity for cancer classification. Intriguingly, the scores of five CA samples (CA1, 3, 4, 11, and 16) when evaluated as test sets are within the range of scores when they were evaluated as part of the training set. With Golub's method, however, the test set-associated score for each sample was always the lowest value obtained. These findings strongly suggest that Golub's method is more dependent on the training set applied than is ADMS. Other evidence of the advantages of ADMS is that the scores of two CA samples (CA7 and CA14) with above five CA samples when evaluated as test set in ADMS were located within the interval of 1% significance level of the 15 scores in each training set, whereas there was no such samples when Golub's method was used. The two methods cannot be compared directly because of the differences in the evaluation scores. However, both scores ranged from -1 to 1 and the positive scores, at least, have the same meaning (the sample is classified as cancerous).

The 135 known genes among the 335 clones selected were categorized according to one of six cellular functions: apoptosis, cell adhesion, cell cycle, signal transduction, gene expression, and miscellaneous (Fig. 5). Many of the expression profiles we obtained agreed with those reported in the literature. Of the 10 apoptosis-related genes, expression of *Bcl2* was consistently higher in adenomas than in carcinomas [14]. Of the 15 cell-adhesive proteins, catenin was down-regulated in the CA and

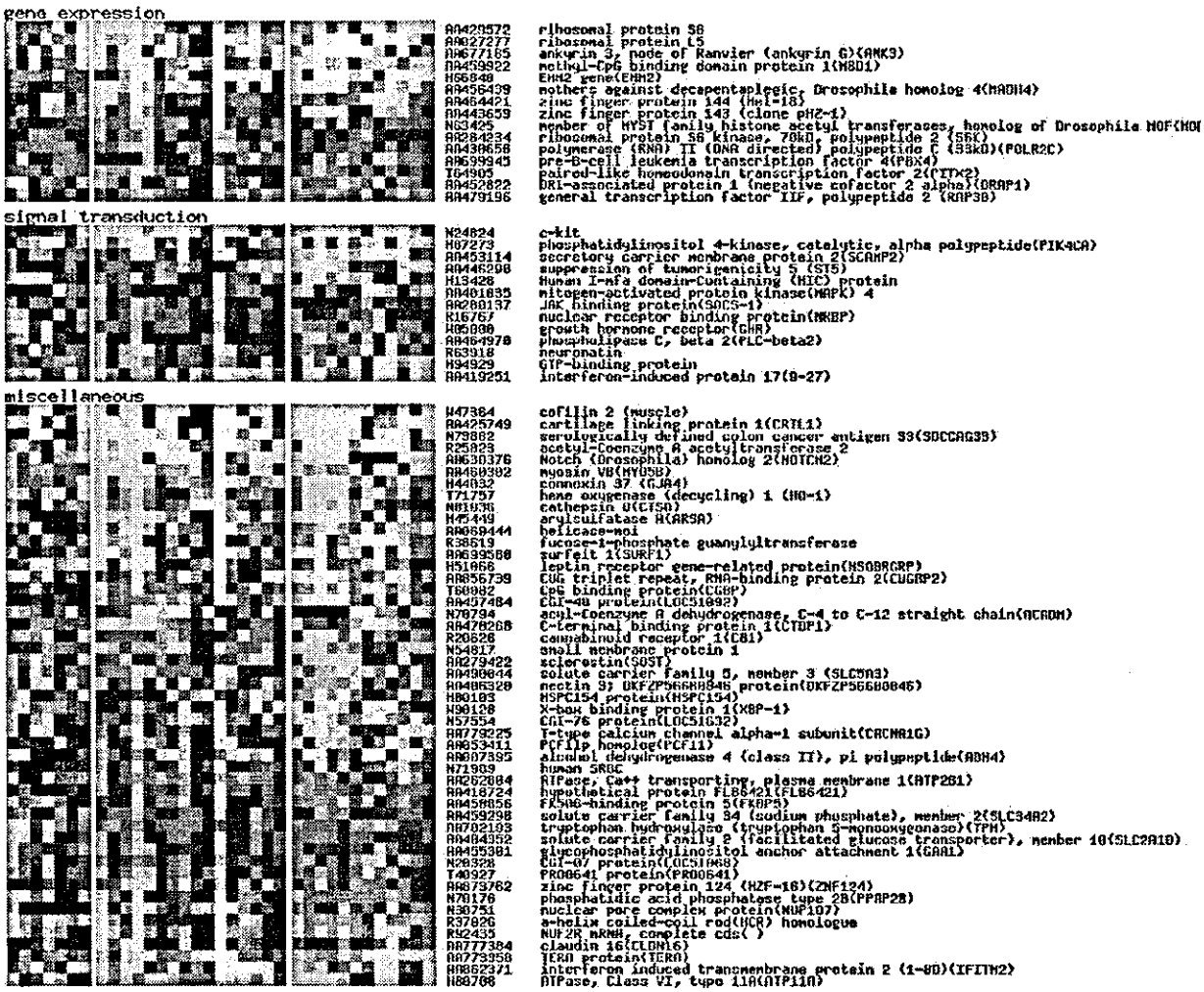

Fig. 5. (*continued*)

metastasis samples. This finding coincided well with a previous report showing that down-regulation of catenin in colon cancer may be associated with metastasis and poor clinical outcome [15]. MUC2 gene is also included in this category. MUC2 encodes intestinal type secretary mucin produced by Goblet's cells. It has been reported that up-regulation of MUC2 is observed in adenoma whereas the gene is not up-regulated in colon cancer unless it is a mucinous type [16]. In the category of cell cycle, *Gas*1, a membrane-associated protein and induces G0 to S phase transition by wild p53 dependent and independent manner was down-regulated in cancer, indicating uncontrolled cell growth [17,18]. TACC3 was reported to be over-expressed in cancer cell line and interact with microtubules in mitosis. This gene is also up-regulated in cancer suggesting active cell division. Cyclin E1 [19], MYBL2 (v-myb avian myeloblastosis viral oncogene homolog-like 2) is also up-regulated in cancer as have been reported in the literature. MYBL2 is a cell-cycle regulated phosphoprotein involved in cell cycle and located on human chromosome 20q13. Amplification of this region has been reported to be involved in malignant carcinoma [20].

During the actual diagnosis of the carcinoma state in light of the multigene expression signature using microarray data, it may not be necessary to adhere to the minimal gene set to diagnose the carcinoma state. In this sense, we did not focus on the identification of the minimal genes set, rather focused on accurately assigning an unknown sample according to its relatedness to the colorectal carcinoma state.

In principle, our method can be used to predict prognosis for a patient. Takahashi et al. [21] could assign patients with renal cell carcinoma to a high- or low-risk group by comparing the expression profile with data regarding the 5-year survival rate. However, in general, it is difficult to set a threshold for discriminating two such groups. Our ADMS method can provide a new measure for the prediction of prognosis.

In summary, our ADMS method showed 100% sensitivity for carcinoma classification, a potential for screening high-risk samples of adenoma, and robustness in the evaluation. In the future, we would like to further decrease the method's dependency on the training set used. ADMS was designed to assess relatedness to a carcinoma state but can be applied to various types of tumors and stages.

Acknowledgments

This study has been supported by a Research Grant for the RIKEN Genome Exploration Research Project from the Ministry of Education, Culture, Sports, Science, and Technology of the Japanese Government and ACT-JST (Research and Development for Applying Advanced Computational Science and Technology) of Japan Science and Technology Corporation (JST) to Y. Hayashizaki and by Special Coordination Funds for Promoting Science and Technology from the Ministry of Education, Culture, Sports, Science, and Technology of the Japanese Government to Y. Okazaki. We thank N. Goto, M. Gariboldi, L. Marchioni, T. Kasukawa, H. Bono for technical assistance and helpful discussion.

References

[1] E.R. Fearon, B. Vogelstein, A genetic model for colorectal tumorigenesis, Cell 61 (1990) 759–767.
[2] D.A. Notterman, U. Alon, A.J. Sierk, A.J. Levine, Transcriptional gene expression profiles of colorectal adenoma, adenocarcinoma, and normal tissue examined by oligonucleotide arrays, Cancer Res. 61 (2001) 3124–3130.
[3] K. Forrester, C. Almoguera, K. Han, W.E. Grizzle, M. Perucho, Detection of high incidence of K-ras oncogenes during human colon tumorigenesis, Nature 327 (1987) 298–303.
[4] S.J. Baker, E.R. Fearon, J.M. Nigro, S.R. Hamilton, A.C. Preisinger, J.M. Jessup, P. van Tuinen, D.H. Ledbetter, D.F. Barker, Y. Nakamura, Chromosome 17 deletions and p53 gene mutations in colorectal carcinomas, Science 244 (1989) 217–221.
[5] E.R. Fearon, K.R. Cho, J.M. Nigro, S.E. Kern, J.W. Simons, J.M. Ruppert, S.R. Hamilton, A.C. Preisinger, G. Thomas, K.W. Kinzler, Identification of a chromosome 18q gene that is altered in colorectal cancers, Science 247 (1990) 49–56.
[6] J. Groden, A. Thliveris, W. Samowitz, M. Carlson, L. Gelbert, H. Albertsen, G. Joslyn, J. Stevens, L. Spirio, M. Robertson, Identification and characterization of the familial adenomatous polyposis coli gene, Cell 66 (1991) 589–600.
[7] T.R. Golub, D.K. Slonim, P. Tamayo, C. Huard, M. Gaasenbeek, J.P. Mesirov, H. Coller, M.L. Loh, J.R. Downing, M.A. Caligiuri, C.D. Bloomfield, E.S. Lander, Molecular classification of cancer: class discovery and class prediction by gene expression monitoring, Science 286 (1999) 531–537.
[8] T.S. Furey, N. Cristianini, N. Duffy, D.W. Bednarski, M. Schummer, D. Haussler, Support vector machine classification and validation of cancer tissue samples using microarray expression data, Bioinformatics 16 (2000) 906–914.
[9] A. Ben-Dor, L. Bruhn, N. Friedman, I. Nachman, M. Schummer, Z. Yakhini, Tissue classification with gene expression profiles, J. Compt. Biol. 7 (2000) 559–583.
[10] L.J. van't Veer, H. Dai, M.J. van de Vijver, Y.D. He, A.A. Hart, M. Mao, H.L. Peterse, K. van der Kooy, M.J. Marton, A.T. Witteveen, G.J. Schreiber, R.M. Kerkhoven, C. Roberts, P.S. Linsley, R. Bernards, S.H. Friends, Gene expression profiling predicts clinical outcome of breast cancer, Nature 415 (2002) 530–536.
[11] R. Miki, K. Kadota, H. Bono, Y. Mizuno, Y. Tomaru, P. Carninci, M. Itoh, K. Shibata, J. Kawai, H. Konno, S. Watanabe, K. Sato, Y. Tokusumi, N. Kikuchi, Y. Ishii, Y. Hamaguchi, I. Nishizuka, H. Goto, H. Nitanda, S. Satomi, A. Yoshiki, M. Kusakabe, J.L. DeRisi, M.B. Eisen, V.R. Iyer, P.O. Brown, M. Muramatsu, H. Shimada, Y. Okazaki, Y. Hayashizaki, Delineating developmental and metabolic pathways in vivo by expression profiling using the RIKEN set of 18,816 full-length enriched mouse cDNA arrays, Proc. Natl. Acad. Sci. USA 98 (2001) 2199–2204.
[12] K. Kadota, R. Miki, H. Bono, K. Shimizu, Y. Okazaki, Y. Hayashizaki, Preprocessing implementation for microarray (PRIM): an efficient method for processing cDNA microarray data, Physiol. Genomics 4 (2001) 183–188.
[13] M.R. Emmert-Buck, R.F. Bonner, P.D. Smith, R.F. Chuaqui, Z. Zhuang, S.R. Goldstein, R.A. Weiss, L.A. Liotta, Laser capture microdissection, Science 274 (1996) 998–1001.
[14] H.A. Saleh, G. Khatib, H. Jackson, M. Banerjee, Correlation of *Bcl2* oncoprotein immunohistochemical expression with proliferation index and histopathologic parameters in colorectal neoplasia, Pathol. Oncol. Res. 5 (1999) 274–279.
[15] J.S. Gold, A.B. Reynolds, D.L. Rimm, Loss of p120ctn in human colorectal cancer predicts metastasis and poor survival, Cancer Lett. 132 (1998) 193–201.
[16] M. Blank, E. Klussmann, S. Kruger-Krasagakes, A. Schmitt-Graff, M. Stolte, G. Bornhoeft, H. Stein, P.X. Xing, I.F. McKenzie, C.P. Verstijnen, Expression of MUC2-mucin in colorectal adenomas and carcinomas of different histological types, Int. J. Cancer 59 (1994) 301–306.
[17] E.M. Ruaro, L. Collavin, G. Del Sal, R. Haffner, M. Oren, A.J. Levine, C. Schneider, A proline-rich motif in p53 is required for transactivation-independent growth arrest as induced by *Gas1*, Proc. Natl. Acad. Sci. USA 94 (1997) 4675–4680.
[18] G. Del Sal, E.M. Ruaro, R. Utrera, C.N. Cole, A.J. Levine, C. Schneider, *Gas1*-induced growth suppression requires a transactivation-independent p53 function, Mol. Cell. Biol. 15 (1995) 7152–7160.
[19] T. Sutter, S. Doi, K.A. Carnevale, N. Arber, I.B. Weinstein, Expression of cyclins D1 and E in human colon adenocarcinomas, J. Med. 28 (1997) 285–309.
[20] F. Forozan, E.H. Mahlamaki, O. Monni, Y. Chen, R. Veldman, Y. Jiang, G.C. Gooden, S.P. Ethier, A. Kallioniemi, O.P. Kallioniemi, Comparative genome hybridization analysis of 38 breast cancer cell lines: a basis for interpreting complementary DNA microarray data, Cancer Res. 60 (2000) 4519–4525.
[21] M. Takahashi, D.R. Rhodes, K.A. Furge, H. Kanayama, S. Kagawa, B.B. Haab, B.T. Teh, Gene expression profiling of clear renal cell carcinoma: gene identification and prognostic classification, Proc. Natl. Acad. Sci. USA 98 (2001) 9754–9759.

Quantitative Analyses of Osteopontin mRNA Expression in Human Proximal Tubules Isolated From Renal Biopsy Tissue Sections of Minimal Change Nephrotic Syndrome and IgA Glomerulonephropathy Patients

Jun-Ya Kaimori, MD, Masaru Takenaka, MD, Yasuyuki Nagasawa, MD, Hideaki Nakajima, MD, Masaaki Izumi, MD, Yoshitaka Akagi, MD, Enyu Imai, MD, and Masatsugu Hori, MD

• **Osteopontin (OPN), a secreted phosphoprotein and chemotactic to monocytes/macrophages, is upregulated in renal cortical tubules in a variety of rodent models of renal injury and is believed to possibly have a role in tubulointerstitial injury. We previously reported the establishment of a system for the quantification of messenger RNA (mRNA) expression in isolated rat glomeruli using laser-manipulated microdissection and real-time polymerase chain reaction. This system was applied to human renal biopsy specimens. We quantified OPN mRNA expression in proximal tubules of 5 patients with minimal change nephrotic syndrome (MCNS) and 11 patients with mild immunoglobulin A (IgA) glomerulonephritis. We also examined the correlation between OPN mRNA expression in proximal tubules and clinical data and pathological findings in glomeruli and tubulointerstitial regions. Patients with MCNS showed a positive correlation between OPN mRNA expression in proximal tubules and urinary protein excretion ($r = 0.93$; $P < 0.05$), whereas for patients with IgA glomerulonephritis, logarithmic values of OPN mRNA expression in proximal tubules positively correlated with low urinary protein levels ($r = 0.72$; $P < 0.05$). Pathological changes, ranging from nonexistent to minor, in glomeruli and tubulointerstitium of these patients with mild IgA glomerulonephritis did not significantly correlate with OPN mRNA expression in proximal tubules. In patients with mild IgA glomerulonephritis, OPN mRNA expression in proximal tubules increased exponentially in response to a small amount of urinary protein (<1.2 g/d).**

INDEX WORDS: Laser microdissection; osteopontin (OPN); proximal tubule; immunoglobulin A (IgA) nephropathy; minimal change nephrotic syndrome (MCNS); proteinuria.

THE KIDNEY CONSISTS of different functional units, termed nephron segments, that presumably express different genes. To analyze gene expression in renal tissues, each nephron segment should be isolated, and to collect the requisite tiny samples of tissue structure from histological specimens, several methods have been used.[1-5] Recently, laser-based techniques have come into use, and successful isolation of a specific nephron segment has been reported.

From the Department of Internal Medicine and Therapeutics, Graduate School of Medicine, Osaka University, Osaka, Japan.

Received June 4, 2001; accepted in revised form November 16, 2001.

Supported in part by a Grant-in-Aid for Scientific Research from the Ministry of Education, Science, and Culture; and the Takeda Medical Research Foundation, Yamanouchi Foundation for Research on Metabolic Disorder, Salt Science, Japan.

Address reprint requests to Masaru Takenaka, MD, Department of Internal Medicine and Therapeutics, Graduate School of Medicine (Box A8), Osaka University, 2-2, Yamadaoka, Suita, Osaka, 560-0871, Japan. E-mail: kidney@medone.med.osaka-u.ac.jp

0272-6386/02/3905-0005$35.00/0

doi:10.1053/ajkd.2002.32768

Two types of laser microdissection techniques are available: laser-capture microdissection (LCM) and laser-manipulated microdissection (LMM).[6,7] With the former method, the laser pulse is used to create focal adhesion between a transparent thermoplastic film and the surface of the targeted tissue section.[6] The strong attachment results in guaranteed procurement of the specific tissue region. With the latter method, the fine laser beam makes it possible to cut out micro tissue structures under a microscope without contamination of other components. The laser beam then blows away the laser-microdissected tissues for collection. We used this method to gather glomeruli from histochemical specimens of rat kidney and quantify messenger RNA (mRNA) of the tissue portion by means of real-time polymerase chain reaction (PCR).[8]

Tubulointerstitial injury is believed to be important for the progression of renal disease.[9,10] Several factors, such as osteopontin (OPN),[11,12] macrophage-specific chemoattractant protein,[11] regulated on activation normal T-cell expressed and secreted chemokine,[13] platelet-derived growth factor,[14] insulin-like growth factor-I,[15] and transforming growth fac-

tor-β (TGF-β),[16] are believed to be involved in tubulointerstitial injury.

OPN is a highly acidic, phosphorylated, secreted protein originally believed to be produced only in bone matrix.[17] Recently, OPN protein secretion was identified in various tissues, including tubular epithelium,[18] macrophages,[19] T lymphocytes,[20] and smooth muscle cells.[21] It has been given many different names, such as uropontin, eta-1, bone sialoprotein-1, and secreted phosphoprotein-1.[18] OPN has an arg-gly-asp (RGD) motif, through which it adheres to osteoclasts, osteoblasts, fibroblasts, and smooth muscle and endothelial cells.[22-24]

In a variety of rodent renal disease models, the appearance of OPN has been observed in cortical tubules from the early stage of the disease before monocyte/macrophage accumulation of tubular damage has become apparent. This is followed by recruitment of monocytes/macrophages for infiltration into the interstitium.[12,25-28] These results indicate that OPN is an important mediator of tubulointerstitial disease. In human progressive membranous nephropathy, strong OPN protein expression in tubular epithelial cells has been shown to coincide with interstitial cell infiltration and tubular injury.[29] In human crescentic glomerulonephritis, monocytes and macrophages in glomerular crescents have been reported to secrete OPN.[30] Okada et al[31] used an immunohistological staining method to show that inducible expression of OPN protein in proximal and distal tubules apparently is related to interstitial monocyte recruitment and tubular interstitial changes in immunoglobulin A (IgA) nephropathy and lupus nephritis (World Health Organization type IV).

For the study reported here, we used the laser-based microdissection technique[8] to quantify mRNA expression in human proximal tubules isolated from histological tissue specimens by means of LMM and LCM, as well as real-time PCR. We examined renal biopsy specimens of 5 patients with minimal change nephrotic syndrome (MCNS) and 11 patients with IgA glomerulonephritis by using LMM to cut and collect proximal tubules accurately and without contaminating other tissues. The amount of OPN mRNA expression in proximal tubules isolated from the renal biopsy specimen was successfully quantified. We also studied any correlation between the quantity of OPN mRNA expression and clinical, histopathologic, and immunohistochemical data for OPN.

MATERIALS AND METHODS

Renal Biopsies

Renal biopsy specimens were obtained from 16 patients (5 patients, MCNS; 11 patients, IgA glomerulonephritis) at Osaka University Hospital (Osaka, Japan) during a standard hospitalization for renal biopsy examination. Informed consent for this study was obtained from all subjects. The protocol for this study was approved by the Ethics Committee of the Department of Internal Medicine and Therapeutics, Osaka University Graduate School of Medicine. For RNA analyses, a section of the biopsy specimen was soaked in an RNAlater reagent (Ambion Inc, Austin, TX) soon after the former was obtained. Subsequently, specimens were fixed in 100% ethanol and embedded in 100% paraffin using a standard method. With the permission of the committee and informed consent, we also used normal kidney tissues obtained from nephrectomy specimens of patients with renal cancer.

Selective Tissue Collection by LMM and LCM

Proximal tubules were isolated according to previously described methods.[8] LMM can collect samples of virtually any shape and size between one to several hundred micrometers in diameter by cutting tissue sections from a histological specimen with a strong laser beam.[7] By careful cutting inside the proximal tubular basement membrane, only epithelial cells of the proximal tubule were successfully isolated, presumably without contamination of other nephron segments. We then collected samples by means of LCM. We identified proximal tubules by confirming their brush borders in serial periodic acid–Schiff (PAS)-stained sections. Ten sections of proximal tubules were immediately processed for the following RNA extraction procedures.

Quantification of OPN mRNA Expression by Real-Time PCR

Ten proximal tubules collected by LMM and LCM were treated with proteinase K solution (200 mmol/L of Tris-HCl, pH7.5; 200 mmol/L of NaCl; 1.5 mmol/L of $MgCl_2$; 2% sodium dodecyl sulfate; 500 μg/mL of proteinase K) for 15 minutes at 45°C.[32] Total RNAs were isolated with the aid of Trizol reagent (Life Technologies, Rockville, MD) according to the manufacturer's instructions. The first strand of complementary DNA (cDNA) was synthesized by using the Superscript Preamplification System (Life Technologies) with random hexamers. Excess primers were removed with a Microcon YM-10 (Millipore, Bedford, MA). Quantification of human OPN/glyceraldehyde-3-phosphate dehydrogenase (GAPDH) mRNA was performed by real-time PCR using the ABI Prism 7700 Sequence Detection System (Perkin Elmer Applied Biosystems, San Diego, CA). The TaqMan probe for human OPN sequence was 5′-CGAAGTTTTCACTCCAGTTGTCCCCACA-3′ (accession no. JO4765; 495 to 522 bp). The forward primer

sequence of human OPN was 5′-TCACTGATTTTCCCACG-GACC-3′ (464 to 484 bp), and the reverse was 5′-CCTCGGCCATCATATGTGTCTA-3′ (524 to 545 bp). The human GAPDH TaqMan probe and forward and reverse primers were obtained from TaqMan Human GAPDH Control Reagents (Perkin Elmer Applied Biosystems).

To prepare standard lines for the quantification of mRNA, human GAPDH was cloned by means of PCR. OPN cDNA was provided by Dr Cecilia M. Giachelli (University of Washington, Seattle, WA). The forward primer sequence of human GAPDH was 5′-TCAGCCGCATCTTCTTTT-GCGTCG-3′ (accession no. NM002046; 25 to 48 bp), and the reverse was 5′-TTGTCATGGATGACCTTGGC-CAGG-3′ (552 to 575 bp). Resultant PCR products were cloned and sequenced for confirmation. Relative amounts of OPN and GAPDH mRNA in each sample were calculated in terms of their own standard lines by using real-time PCR (details of these procedures using real-time PCR are described at the Internet site of Perkin Elmer: http://www2.perkin-elmer.com/ab/).

To determine whether there was contamination in collected proximal tubules, we performed reverse transcriptase PCR along with real-time PCR of human Tamm-Horsfall glycoprotein. Primer sequences (accession no. M15881 and M17778) were 5′ TCCAAGTGGTGGAGAATGGG 3′ (forward primer) and 5′ TCCAGCAAACCGGAACATCT3′ (reverse primer). The TaqMan probe for human Tamm-Horsfall glycoprotein was 5′ Fam-CCTCCCAGGGC-CGATTTTCCGT-Tamra 3′.

Immunohistochemistry

Four-micron sections were processed by means of an indirect avidin-biotin immunoperoxidase method (Vectastain ABC kit; Vector Laboratories, Burlingame, CA) using the mouse monoclonal antibody MPIIIB10, which is specific for rat OPN and has been shown to cross-react with human OPN (American Research Products, Belmont, MA) and the murine monoclonal antibody PGM1, directed against CD68 on human macrophages and monocytes (Dako, Carpinteria, CA). The number of CD68-positive cells was determined as described previously[33] to evaluate interstitial monocyte/macrophage infiltration. Ten random cortical fields were counted for CD68-positive cells, using original magnification ×400. Results are shown as the total number of CD68-positive cells per high-power field.

Pathological Examination

Glomerular and tubulointerstitial examinations were performed by two renal pathologists using 1-μm PAS-stained sections from the same renal biopsy specimens. Glomerular injuries of sections were scored semiquantitatively to determine the proportion of mesangial cells that had proliferated and the increase in mesangial matrix.[34,35] Proliferation of mesangial cells observed with light microscopy was classified according to the following scale of 0 to 3: 0, none; 1, proliferation of mesangial cells observed in less than 25% of glomeruli (mild); 2, proliferation of mesangial cells observed in 25% to 75% of glomeruli (moderate); and 3, proliferation of mesangial cells observed in more than 75% of glomeruli (severe). The increase in mesangial matrix was evaluated according to the following scale of 0 to 3: 0, no increase; 1, up to 25% of sclerotic glomeruli affected (mild); 2, 26% to 50% of glomeruli affected (moderate); and 3, more than 50% of glomeruli affected (severe).

Tubulointerstitial injuries were evaluated in terms of interstitial cell infiltration and fibrosis.[34,35] Interstitial cell infiltration was scored according to the following scale of 0 to 3: 0, less than 10% of parenchyma cell infiltrated; 1, 10% to 25% of parenchyma cell infiltrated; 2, 26% to 50% of parenchyma cell infiltrated; and 3, more than 50% of parenchyma cell infiltrated. Interstitial fibrosis was evaluated according to the following scale of 0 to 3: 0, interstitial fibrosis in up to 5% of the cortical area; 1, interstitial fibrosis in 6% to 25% of the cortical area; 2, interstitial fibrosis in 26% to 50% of the cortical area; and 3, interstitial fibrosis in greater than 50% of the cortical area. The presence of interstitial monocytes/macrophages was evaluated in terms of CD68-positive cell infiltration. Scores were averaged, although they were virtually identical.

Clinical Data Presentation

Urinary protein excretion (in grams per day), serum creatinine (in milligrams per deciliter), urinary protein-creatinine ratio, creatinine clearance (in milliliters per minute), body weight (in kilograms), blood pressure (in millimeters of mercury), sex, and age at the time of renal biopsy are shown.

RESULTS

Accurate Human Proximal Tubule Collection by LMM and LCM to Quantify Segment-Specific mRNA Expression Isolated From Historic Specimens

To evaluate mRNA expression in nephron segments, we applied an established method to isolate human proximal tubules from histological specimens.[8] By careful cutting inside their basement membrane by means of LMM, only epithelial cells of proximal tubules could be isolated with virtually no contamination of other components. Cells were then collected by means of LCM (Fig 1). We could identify proximal tubules by confirming their brush borders in serial PAS-stained sections. OPN gene expression in human proximal tubules also was measured because OPN has been reported to be an important mediator of tubulointerstitial injuries in a variety of animal disease models,[12,25,27,28,36] as well as in human progressive membranous nephropathy.[29]

In normal renal tissue taken from tumor-containing kidneys, OPN protein expression has been reported to vary among specimens.[37] We therefore collected 10 proximal tubules to average any variability of OPN mRNA expression.

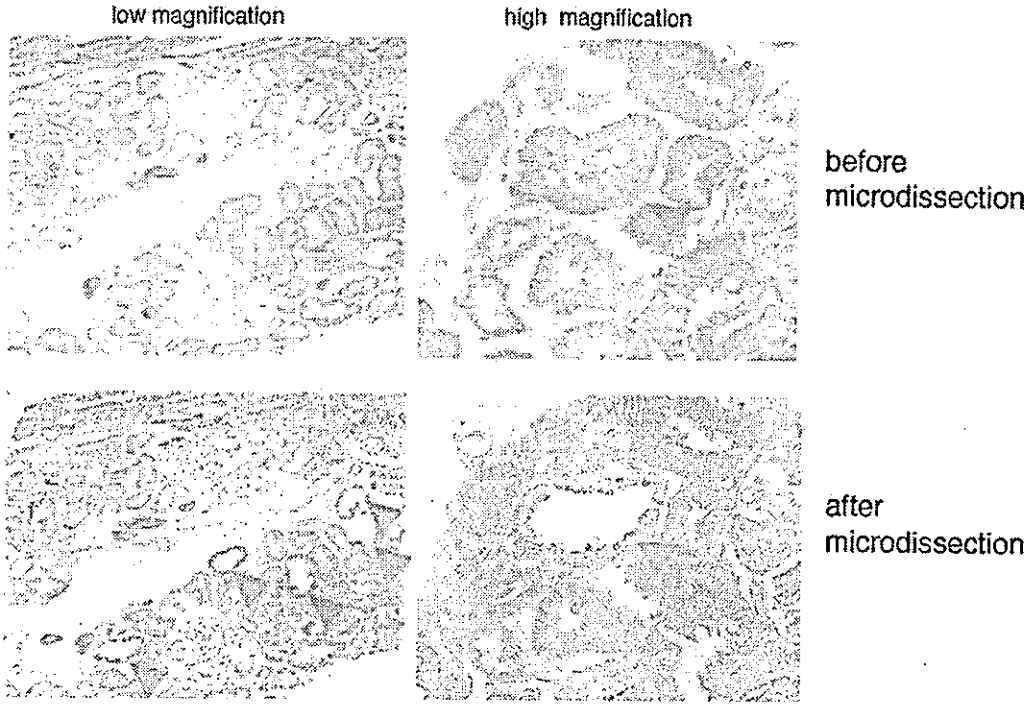

Fig 1. Representative photographs of a human renal biopsy specimen before and after laser microdissection. By carefully cutting inside the proximal tubular basement membrane, only epithelial cells of the proximal tubule were successfully isolated without contamination using LMM. They were collected by means of LCM. Microdissected and collected proximal tubules are shown by arrowheads. (High original magnification ×400; low original magnification ×40.)

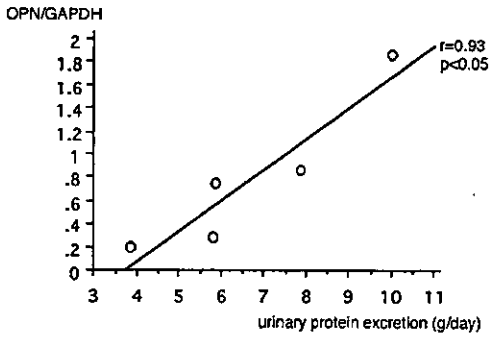

Fig 2. Correlation between OPN/GAPDH and urinary protein excretion in five patients with MCNS. Each dot shows the OPN/GAPDH value and quantity of urinary protein excretion in each patient with MCNS. The correlation was statistically significant ($P < 0.05$).

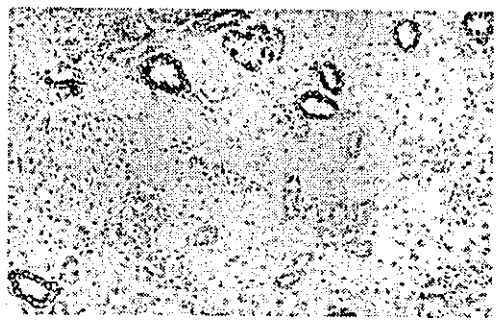

Fig 3. Representative photograph of immunohistochemical staining for OPN in a human renal biopsy section of patient 2 with MCNS. These staining patterns were virtually identical to those reported in normal kidney. The section was 4-μm thick.

Table 1. Data for Patients With MCNS and IgA Nephropathy

Patient No.	Age (y)/ Sex	BW (kg)	s-Cr (mg/dL)	CCr (mL/min)	BP (mm Hg)	Mean U-Prot (g/d)	U-Prot/U-Cr	OPN/GAPDH	SI*
MCNS									
1	26/F	58.9	0.6	103	90/60	3.9	4.1	0.197	0.095
2	23/F	46.6	0.6	95	132/80	5.9	6.8	0.749	0.016
3	38/F	69.9	0.6	87.9	113/75	7.9	7.5	0.867	0.097
4	26/F	44.7	0.4	81	86/52	10	10.9	1.864	0.127
5	59/F	42.5	0.6	88	102/84	5.8	5.9	0.281	0.098
IgA glomerulonephritis									
1	17/M	54.0	0.9	156	124/68	0.18	0.16	0.14	ND
2	34/F	46.4	1.2	63	102/70	0.79	0.81	1.31	ND
3	45/M	67.3	0.9	73.6	115/72	0.48	0.50	0.69	ND
4	32/M	55.5	1.0	76.9	116/78	0.72	0.75	4.86	ND
5	52/F	47.6	0.6	92	132/70	0.77	0.85	0.18	ND
6	55/M	89.2	0.8	111	138/84	0.67	0.61	0.55	ND
7	29/F	75.4	0.6	120	102/72	0.15	0.10	0.05	ND
8	24/F	59.5	0.6	120	102/74	0.85	0.78	0.25	ND
9	48/M	56.2	0.9	104	128/62	0.30	0.17	0.29	ND
10	26/F	54.1	0.4	132	96/63	1.20	0.95	4.64	ND
11	27/M	68.5	0.7	165	120/55	0.79	0.66	1.01	ND

Abbreviations: BW, body weight; s-Cr, serum creatinine; CCr, creatinine clearance; BP, blood pressure; U-prot, urinary protein; OPN/GAPDH, osteopontin mRNA/GAPDH mRNA; SI, selectivity index; ND, not detected.

*Urinary transferrin was not detected in patients with IgA glomerulonephritis; thus, SIs were not measured.

Total mRNA was extracted from the 10 proximal tubules and converted to cDNA by reverse transcriptase reaction, described in Materials and Methods. Human GAPDH and target mRNA were quantified by means of real-time PCR,[8] and expression ratios of OPN-GAPDH mRNA were determined. Clinical data and OPN mRNA expression values are listed in Table 1. OPN/GAPDH expression in proximal tubules obtained from nephrectomy specimens of patients with renal cancer was less than 0.04.

To determine whether there was contamination of other nephron segments, we performed real-time PCR for human Tamm-Horsfall glycoprotein. Because no PCR products were detected in mRNA extracted from isolated proximal tubules using the laser-based microdissection method (data not shown), we assumed there was virtually no contamination of distal tubules. Proximal tubules of normal tissues obtained from nephrectomy specimens were isolated, and OPN/GAPDH mRNA was determined as described in Materials and Methods. OPN/GAPDH expression of normal proximal tubules was 0.03, 0.01, 0.04, and 0.01, indicating they were less than the lowest value of patients.

Correlation of Urinary Protein Excretion and OPN mRNA Expression in Patients With MCNS

We first examined clinical profiles of the five patients with MCNS, including OPN mRNA expression (Table 1), and found a positive correlation between OPN mRNA expression and urinary protein (Fig 2). This result seems to agree with results of experiments using disease models.[11,27] OPN mRNA expression in proximal tubules of patients with MCNS was upregulated in proportion to the quantity of urinary protein.

To confirm OPN expression further, OPN was subjected to immunohistochemical analyses. Staining patterns of these five patients were virtually identical to those of normal human kidney tissue in which only collecting ducts and distal tubules were positively stained (Fig 3). Their OPN mRNA expression could be quantified using LMM and PCR methods. Immunohistochemical analyses using anti-CD68 antibody showed that monocytes or macrophages were not present in the interstitium of patients with MCNS (data not shown).

Correlation of Urinary Protein Excretion and OPN mRNA Expression in Patients With IgA Glomerulonephritis

We examined OPN mRNA expression in proximal tubules, pathological evaluation results, and urinary protein levels in the 11 patients with IgA glomerulonephritis. Patients with IgA glomerulonephritis listed in Table 1 showed no or minor pathological changes and urinary protein excretion less than 1 g/d. As shown in Fig 4, there was a positive correlation between the logarithmic value of OPN mRNA expression in proximal tubules and urinary protein. Patients with IgA glomerulonephritis with proteinuria less than 1 g/d of protein showed exponential upregulation of OPN mRNA in proximal tubules. No other clinical data, including blood pressure and renal function, showed a significant correlation with OPN mRNA expression (data not shown).

In Table 1, urinary protein-creatinine ratios and body weight are shown for a comparison among individuals of different masses, again showing no significant difference. Typical immunohistochemical stainings of OPN are shown in Fig 5. We found that cortical tubules of patient 4, who had OPN expression values greater than 4, were diffusely stained. Conversely, the staining pattern of patient 7 (OPN expression value, 0.05), as well as those of other patients, looked similar to reported normal expression patterns in the kidney.[37] OPN expression levels of normal proximal tubules obtained from nephrectomy specimens were quantified. Values were less than the lowest value of patients. By using laser-based microdissection and the mRNA quantifying procedure, we thus could detect differences in OPN mRNA expression in proximal tubules, even if OPN immunostaining could not be clearly identified.

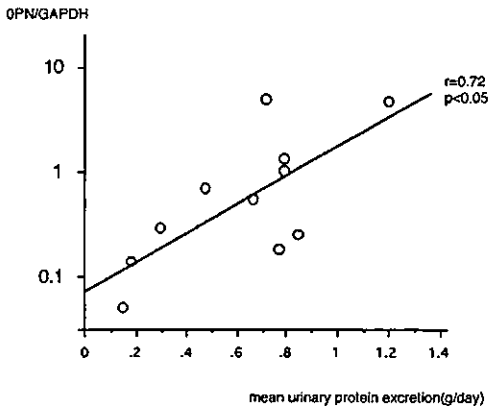

Fig 4. The correlation between the logarithmic value of OPN/GAPDH and urinary protein excretion in patients with IgA glomerulonephritis was statistically significant ($P < 0.05$).

Fig 5. Immunohistochemical staining for OPN in human renal biopsy specimens from patients with IgA glomerulonephritis. (A) OPN-positive stains were diffusely detected in cortical tubules, including proximal tubules of patient 4 with IgA glomerulonephritis. (B) Staining patterns of patient 7 with IgA glomerulonephritis were similar to those reported in normal kidney.

Correlation of OPN mRNA Expression and Pathological Evaluation, Including Glomerular or Tubulointerstitial Injury, in Patients With IgA Glomerulonephritis

We examined OPN mRNA expression in proximal tubules of patients with IgA glomerulonephritis with respect to pathological evaluations of glomerular and tubulointerstitial injury. Glomerular injuries were evaluated in terms of proliferation of mesangial cells and increase in mesangial matrix. Tubulointerstitial injury was assessed in terms of interstitial cell infiltration and fibrosis.

We ranked proliferation of mesangial cells, increase in mesangial matrix, interstitial cell infiltration, and interstitial fibrosis on a scale of 0 to 3 according to the pathological score for each category, described in Materials and Methods.[34,35]

OPN mRNA expression in proximal tubules of patients with moderate-stage IgA glomerulonephritis entered onto our study did not correlate with pathological evaluations of glomerular or tubulointerstitial injury (Fig 6). To examine the correlation between interstitial monocyte/macrophage infiltration and OPN mRNA expression in proximal tubules of patients with IgA glomerulonephritis, we performed immunochemical analyses of monocytes/macrophages using anti-CD68 antibody PGM1 and counted the number of CD68-positive infiltrated interstitial cells. No significant correlation was found between the number of CD68-positive interstitial cells and OPN mRNA expression in proximal tubules (data not shown).

DISCUSSION

LMM, together with real-time PCR,[8] was used to quantify OPN mRNA expression in proximal tubules of human renal biopsy sections. We succeeded in isolating proximal tubules by means of the laser microdissection method and quantifying OPN mRNA expression level in 10 proximal tubules of 10-μm thick human renal biopsy specimens. This laser-based procedure previously enabled us to quantify TGF-β mRNA expression in rat glomeruli of an anti-Thy 1 glomerulonephritis model.[8] The same method allowed us to detect and quantify mRNA expression in proximal tubules of renal biopsy specimens, and this method seemed to be more sensitive than immunohistochemical analyses. We could detect differences in OPN mRNA expression in proximal

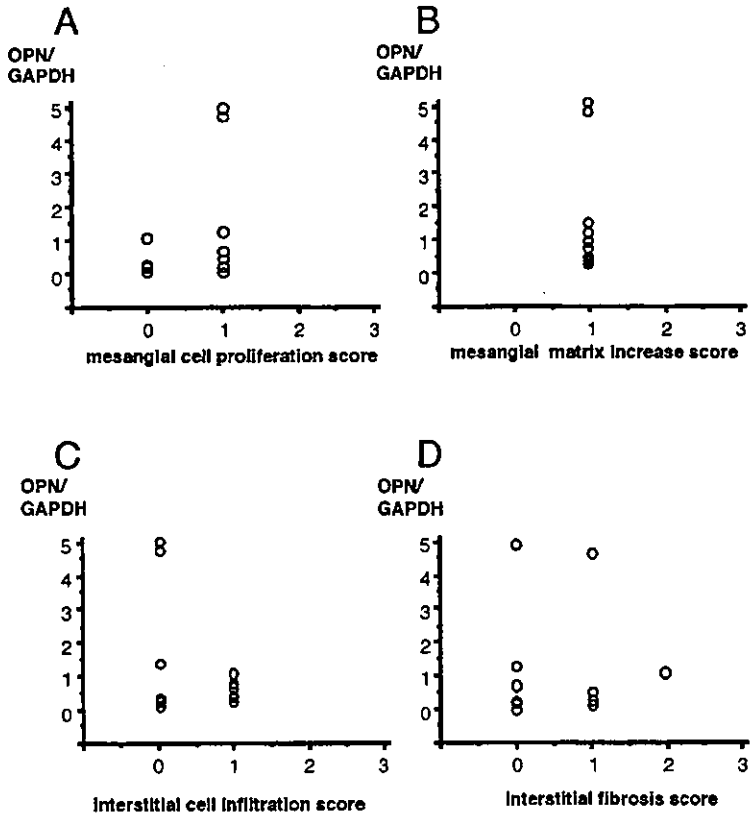

Fig 6. Evaluation between OPN mRNA expression and pathological findings. The amount of OPN mRNA expression in proximal tubules of patients with IgA glomerulonephritis was evaluated by (A) proliferation of mesangial cells, (B) increase in mesangial matrix, (C) interstitial cell infiltration, and (D) interstitial fibrosis. There seemed to be no significant correlations.

tubules of patients even if results of OPN immunostaining were not clear. This laser-based procedure also enabled us to simultaneously perform quantification of gene expression and pathological evaluation by using the same renal biopsy tissue specimen. However, in situ hybridization would be preferable for the localization of mRNA expression. This laser-based procedure thus may be suitable for the quantification of mRNA expression in highly restricted and very small sections of tissue specimens.

For this study, we selected OPN as an important mediator of tubulointerstitial disease and quantified its mRNA expression in proximal tubules. OPN, a phosphoprotein, creates strong adhesion to macrophages in vitro[20,38] and exerts chemotactic activity on macrophages. Subcutaneous infusion of OPN resulted in a cellular infiltrate consisting primarily of macrophages.[38] Recently, many studies using in situ hybridization and immunohistochemistry for various renal injury models have reported that upregulation of OPN was observed in proximal tubules, and this upregulation was related to interstitial cell infiltration and fibrosis.[12,26,28,36] Patients with progressive idiopathic membranous nephropathy and IgA glomerulonephritis showed overexpression of OPN in proximal tubular epithelial cells assessed by immunohistochemistry, and this overexpression was associated with an interstitial accumulation of mononuclear cells.[29,31] In normal rat kidney, OPN was found only in distal tubules,[39] whereas in human kidney, OPN mRNA and protein were identified in distal tubules, collecting ducts, and transitional epithelium of the renal pelvis.[40]

OPN mRNA levels significantly increased in proportion to the quantity of urine protein in the rat kidney with overload proteinuria[11] and puromycin aminonucleoside nephrosis.[27] These reports suggested that proteinuria might cause increased OPN mRNA expression in kidney. We therefore gave special attention to the correlation of urinary protein excretion and OPN mRNA expression in proximal tubules of patients with MCNS and IgA glomerulonephritis. OPN expression in five patients with MCNS was measured successfully using the laser microdissection real-time PCR method, and their immunostaining patterns were virtually identical to those of normal human kidney tissues. However, there was a positive correlation between OPN expression and urinary protein excretion in patients with MCNS (Fig 2). These results seem to agree with those obtained in proteinuria rat models.[11,27]

Conversely, a small quantity of urinary protein (<1.2 g/d) was associated with the exponential upregulation of OPN mRNA expression in proximal tubules of patients with IgA glomerulonephritis. These results may explain the importance of a small quantity of urinary protein in the disease course of IgA glomerulonephritis.

There may be several explanations for the difference in expression patterns of OPN mRNA in proximal tubules between patients with MCNS and IgA glomerulonephritis. Inflammation in glomeruli of patients with IgA glomerulonephritis may cause the secretion of various cytokines, resulting in a remarkable increase in expression of OPN mRNA in proximal tubules. OPN expression in cultured rat renal epithelial cells increased 7.0 to 8.5 times as much as in control subjects in response to several cytokines, such as TGF-β and epidermal growth factor.[41] Angiotensin II infusion has been reported to enhance OPN expression in rat cortical tubules.[28]

Another possible explanation of the difference is the low selectivity of urine protein in patients with IgA glomerulonephritis.[42,43] Urinary protein in patients with MCNS is mainly albumin, whereas several kinds of proteins other than albumin are assumed to be contained in urine of patients with IgA glomerulonephritis. Various proteins have been shown to be involved in tubulointerstitial injury. Transferrin[44,45] and lipoproteins[46,47] are reportedly cytotoxic. Furthermore, the possible role of complement components in tubulointerstitial injury was emphasized in recent studies.[48,49] These findings may help explain our observation of the exponential increase in OPN mRNA expression in proximal tubules of patients with IgA glomerulonephritis.

Patients with IgA glomerulonephritis with urinary protein excretion less than 1 g/d on this study showed pathological changes ranging from nonexistent to minor. OPN immunohistochemistry showed diffuse staining of tubules of only those patients with OPN mRNA expression greater than 1. In other patients, OPN staining patterns were similar to those of normal human kidney. This suggests that laser-based microdissection combined with the real-time PCR proce-

dure may be more sensitive than immunohistochemistry in terms of identification of a particular gene product. We did not observe a correlation between pathological evaluations of tubulointerstitial injury, monocyte/macrophage infiltration to the interstitium, and OPN mRNA expression of mild IgA glomerulonephritis. This may be because the quantity of OPN expression detected with this method is too small to recruit monocytes/macrophages to the interstitium or OPN secretion may be insufficient. The first patient joined this program approximately 18 months ago and has shown no clinical changes to date. Further studies are required to address the question of whether the amount of OPN gene expression in proximal tubules correlates with the prognosis for pathological changes in IgA glomerulonephritis.

If results of the Human Genome Project enable us to identify the key player genes of the progression of human tubulointerstitial injury, we may be able to use this method for a more accurate prognosis of kidney disease.

ACKNOWLEDGMENT

The authors thank Naoko Horimoto, Sonoe Watanabe, and Masako Kishihata for expert technical support; Dr Cecilia M. Giachelli (University of Washington, Seattle, WA) for providing human OPN cDNA; and Dr Shiro Takahara and Dr Kiyomi Matsumiya in the Division of Urology.

REFERENCES

1. Burg MB, Grantham J, Abramow M, Orloff J, Schafer JA: Preparation and study of fragments of single rabbit nephrons. J Am Soc Nephrol 8:675-683, 1977

2. Wright PA, Burg MB, Knepper MA: Microdissection of kidney tubule segments. Methods Enzymol 191:226-231, 1990

3. Gupta SK, Douglas-Jones AG, Morgan JM: Microdissecton of stained archival tissue. Mol Pathol 50:218-220, 1997

4. Going JJ, Lamb RF: Practical histological microdissection for PCR analysis. J Pathol 179:121-124, 1996

5. Youngson BJ, Anelli A, Van Zee KJ, Borgen PI, Norton L, Rosen PP: Microdissection and molecular genetic analysis of HER2/neu in breast carcinoma. Am J Surg Pathol 19:1354-1358, 1995

6. Emmert-Buck MR, Bonner RF, Chuaqui RF, Zhuang Z, Goldstein SR, Weiss RA, Liotta LA: Laser capture microdissection. Science 274:998-1001, 1996

7. Schutze K, Lahr G: Identification of expressed genes by laser-mediated manipulation of single cells. Nat Biotechnol 16:737-742, 1998

8. Nagasawa Y, Takenaka M, Matsuoka Y, Imai E, Hori M: Quantitation of mRNA expression in glomeruli using laser-manipulated microdissection and laser pressure catapulting. Kidney Int 57:717-723, 2000

9. Nath KA: Tubulointerstitial changes as a major determinant in the progressive renal damage. Am J Kidney Dis 20:1-17, 1992

10. Bohle A, van Gise H, Mackensen-Haen S, Stark-Jakob B: The obliteration of the postglomerular capillaries and its influence upon the function of both glomeruli and tubuli. Klin Wochenschr 59:1043-1051, 1981

11. Eddy AA, Giachelli CM: Renal expression of genes that promote interstitial inflammation and fibrosis in rats with protein-overload proteinuria. Kidney Int 47:1546-1557, 1995

12. Pichler R, Giachelli CM, Lombardi D, Pippin J, Gordon K, Alpers CE, Schwarz SM, Johnson RJ: Tubulointerstitial disease in glomerulonephritis: Potential role of osteopontin. Am J Pathol 144:915-926, 1994

13. Heeger P, Wolf G, Meyers C, Sun MJ, O'Farrell SC, Krensky AM, Neilson EG: Isolation and characterization of cDNA from renal tubular epithelium encoding murine RANTES. Kidney Int 41:220-225, 1992

14. Tang WW, Ulich TR, Lacey DL, Hill DC, Qi M, Kaufman SA, Van GY, Tarpley JE, Yee JS: Platelet-derived growth factor-BB induces renal tubulointerstitial myofibroblast formation and tubulointerstitial fibrosis. Am J Pathol 148:1169-1180, 1996

15. Hirschberg R: Bioactivity of glomerular ultrafiltrate during heavy proteinuria may contribute to renal tubulointerstitial lesions: Evidence for a role for insulin-like growth factor I. J Clin Invest 98:116-124, 1996

16. Yamamoto T, Noble NA, Miller DE, Border WA: Sustained expression of TGF-beta1 underlies development of progressive kidney fibrosis. Kidney Int 45:916-927, 1994

17. Prince CW, Oosawa T, Butler WT, Tomana M, Brown AS, Brown M, Schrohenlohr RE: Isolation, characterization and biosynthesis of a phosphorylated glycoprotein from rat bone. J Biol Chem 262:2900-2907, 1987

18. Butler WT: The nature and significance of osteopontin. Connect Tissue Res 23:123-136, 1989

19. Miyazaki Y, Setoguchi M, Yoshida S, Higuchi Y, Akizuki S, Yamamoto S: The mouse osteopontin gene: Expression in monocytic lineages and complete nucleotide sequence. J Biol Chem 265:14432-14438, 1990

20. Patarca R, Freeman GJ, Singh RP, Wei F-Y, Durfee T, Blattner F, Regnier DC, Kozak CA, Mock BA, Morse HC III, Jerrells TR, Cantor H: Structural and functional studies of the early T lymphocyte activation 1(Eta-1) gene. J Exp Med 170:145-161, 1989

21. Giachelli CM, Bae N, Lombardi D, Majesky M, Schwartz S: Molecular cloning and characterization of 2B7, a rat mRNA which distinguishes smooth muscle cell phenotypes in vitro and is identical to osteopontin (secreted phosphoprotein I 2aR). Biochem Biophys Res Commun 177:867-873, 1991

22. Liaw L, Almeida M, Hart CE, Schwartz SM, Giachelli CM: Osteopontin promotes vascular cell adhesion and spreading and is chemotactic for smooth muscle cells in vitro. Circ Res 74:214-224, 1994

23. Oldberg A, Franzen A, Heinegard D: Cloning and sequence analysis of rat bone sialoprotein (osteopontin)

cDNA reveals an Arg-Gly-Asp cell binding sequence. Proc Natl Acad Sci U S A 83:8819-8823, 1986

24. Somerman MJ, Fisher LW, Foster RA, Sauk JJ: Human bone sialoprotein I and II enhance fibroblast attachment in vitro. Calcif Tissue Int 43:50-53, 1988

25. Persy VP, Verstrepen WA, Ysebaert DK, De Greef KE, De Broe ME: Differences in osteopontin up-regulation between proximal and distal tubules after renal ischemia/reperfusion. Kidney Int 56:601-611, 1999

26. Young BA, Burdmann EA, Johnson RJ, Alpers CE, Giachelli CM, Eng E, Andoh T, Bennett WM, Couser WG: Cellular proliferation and macrophage influx precede interstitial fibrosis in cyclosporine nephrotoxicity. Kidney Int 48:439-448, 1995

27. Magil AB, Pichler RH, Johnson RJ: Osteopontin in chronic puromycin aminonucleoside nephrosis. J Am Soc Nephrol 8:1383-1390, 1997

28. Giachelli CM, Pichler R, Lombardi D, Denhart DT, Alpers CE, Schwartz SM, Johnson RJ: Osteopontin expression in angiotensin II-induced tubulointerstitial nephritis. Kidney Int 45:515-524, 1994

29. Mezzano SA, Droguett MA, Burgos ME, Ardiles LG, Aros CA, Caorsi I, Egido J: Overexpression of chemokines, fibrogenic cytokines, and myofibroblasts in human membranous nephropathy. Kidney Int 57:147-158, 2000

30. Hudkins KL, Giachelli CM, Eitner F, Couser WG, Johnson RJ, Alpers CE: Osteopontin expression in human crescentic glomerulonephritis. Kidney Int 57:105-116, 2000

31. Okada H, Moriwaki K, Konishi K, Kobayashi T, Sugahara S, Nakamoto H, Saruta T, Suzuki H: Tubular osteopontin expression in human glomerulonephritis and renal vasculitis. Am J Kidney Dis 36:498-506, 2000

32. Masuda N, Ohnishi T, Kawamoto S, Monden M, Okubo K: Analysis of chemical modification of RNA from formalin-fixed samples and optimization of molecular biology applications for such samples. Nucleic Acids Res 27: 4436-4443, 1999

33. Giachelli CM, Lombardi D, Johnson RJ, Murry CE, Almeida M: Evidence for a role of osteopontin in macrophage infiltration in response to pathological stimuli in vivo. Am J Pathol 152:353-358, 1998

34. Oka K, Imai E, Moriyama T, Akagi Y, Ando A, Hori M, Okuyama A, Toki K, Kyo M, Kokado Y, Takahara S: A clinicopathological study of IgA nephropathy in renal transplant recipients: Beneficial effect of angiotensin-converting enzyme inhibitor. Nephrol Dial Transplant 15:689-695, 2000

35. Racusen LC, et al: The Banff 97 working classification of renal allograft pathology. Kidney Int 55:713-723, 1999

36. Diamond JR, Kees-Forts D, Ricardo SD, Pruznak A, Eufemio M: Early and persistent up-regulated expression of renal cortical osteopontin in experimental hydronephrosis. Am J Pathol 146:1455-1466, 1995

37. Hudkins KL, Giachelli CM, Cui Y, Couser WG, Johnson RJ, Alpers CE: Osteopontin expression in fetal and mature human kidney. J Am Soc Nephrol 10:444-457, 1999

38. Singh RP, Patarca R, Schwartz J, Singh P, Cantor H: Definition of a specific interaction between the early T lymphocyte activation 1 (Eta-1) protein and murine macrophages in vitro and its effect upon macrophages in vivo. J Exp Med 171:1931-1942, 1990

39. Nomura S, Wills AJ, Edwards DR, Heath JK, Hogan BL: Developmental expression of 2ar (osteopontin) and SPARC (osteonectin) RNA as revealed by in situ hybridization. J Cell Biol 106:441-450, 1988

40. Brown LF, Berse B, Van De Water L, Papadopoulos-Sergiou A, Peerruzi CA, Manseau EJ, Dvorak HF, Senger DR: Expression and distribution of osteopontin in human tissues: Widespread association with luminal epithelial surfaces. Mol Biol Cell 3:1169-1180, 1992

41. Malyankar UM, Almeida M, Johnson RJ, Pichler RH, Giachelli CM: Osteopontin regulation in cultured rat renal epithelial cells. Kidney Int 51:1766-1773, 1997

42. Woo KT, Lau YK, Yap HK, Lee GS, Chiang GS, Lim CH: Protein selectivity: A prognostic index in IgA nephritis. Nephron 52:300-306, 1989

43. Ikegaya N, Nagase M, Honda N, Kumagai H, Hishida A: Correlation between histologic features and glomerular permeability in membranous nephropathy and immunoglobulin A nephropathy. J Lab Clin Med 123:94-101, 1994

44. Howard RL, Buddington B, Alfrey AC: Urinary albumin, transferrin and iron excretion in diabetic patients. Kidney Int 40:923-926, 1991

45. Alfrey AC, Froment DH, Hammond WS: Role of iron in the tubulo-interstitial injury in nephrotoxic serum nephritis. Kidney Int 36:753-759, 1989

46. Kees-Folts D, Sadow JL, Schreiner GF: Tubular catabolism of albumin is associated with the release of an inflammatory lipid. Kidney Int 45:1697-1709, 1994

47. Thomas ME, Schreiner GF: Contribution of proteinuria to progressive renal injury: Consequences of tubular uptake of fatty acid bearing albumin. Am J Nephrol 13:385-398, 1993

48. Nomura A, Morita Y, Maruyama S, Hotta N, Nadai M, Wang L, Hasegawa T, Matsuo S: Role of complement in acute tubulointerstitial injury of rats with aminonucleoside nephrosis. Am J Pathol 151:539-547, 1997

49. Morita Y, Nomura A, Yuzawa Y, Nishikawa K, Hotta N, Shimizu F, Matsuo S: The role of complement in the pathogenesis of tubulointerstitial lesions in rat mesangial proliferative glomerulonephritis. J Am Soc Nephrol 8:1363-1372, 1997

J Hum Genet (2002) 47:532–538

ORIGINAL ARTICLE

**Fumihiro Akiyama · Toshihiro Tanaka · Ryo Yamada
Yozo Ohnishi · Tatsuhiko Tsunoda · Shiro Maeda
Takashi Takei · Wataru Obara · Kyoko Ito
Kazuho Honda · Keiko Uchida · Ken Tsuchiya
Kosaku Nitta · Wako Yumura · Hiroshi Nihei
Takashi Ujiie · Yutaka Nagane · Satoru Miyano
Yasushi Suzuki · Tomoaki Fujioka · Ichiei Narita
Fumitake Gejyo · Yusuke Nakamura**

Single-nucleotide polymorphisms in the class II region of the major histocompatibility complex in Japanese patients with immunoglobulin A nephropathy

Received: May 28, 2002 / Accepted: July 4, 2002

Abstract Immunoglobulin A nephropathy (IgAN) is a form of chronic glomerulonephritis of unknown etiology and pathogenesis. Immunogenetic studies have not conclusively indicated that human leukocyte antigen (HLA) is involved. As a first step in investigating a possible relationship between HLA class II genes and IgAN, we analyzed the extent of linkage disequilibrium (LD) in this region of chromosome 6p21.3 in a Japanese test population and found extended LD blocks within the class II locus. We designed a case-control association study of single-nucleotide polymorphisms (SNPs) in each of those LD blocks, and determined that SNPs located in the *HLA-DRA* gene were significantly associated with an increased risk of IgAN (P = 0.000001, odds ratio = 1.91 [95% confidence interval 1.46–2.49]); SNPs in other LD blocks were not. Our data imply that some haplotype of the *HLA-DRA* locus has an important role in the development of IgAN in Japanese patients.

Key words Single-nucleotide polymorphism · IgA nephropathy · Linkage disequilibrium · HLA class II · *HLA-DRA*

F. Akiyama · W. Obara · S. Miyano · Y. Nakamura
Human Genome Center, The Institute of Medical Science, University of Tokyo, Tokyo, Japan

F. Akiyama · I. Narita · F. Gejyo
Division of Clinical Nephrology and Rheumatology, Niigata University Graduate School of Medical and Dental Sciences, Niigata, Japan

T. Tanaka · Y. Ohnishi
Laboratory for Cardiovascular Diseases, SNP Research Center, The Institute of Physical and Chemical Research (RIKEN), Tokyo, Japan

R. Yamada
Laboratory for Rheumatic Diseases, SNP Research Center, The Institute of Physical and Chemical Research (RIKEN), Tokyo, Japan

T. Tsunoda
Laboratory for Medical Informatics, SNP Research Center, The Institute of Physical and Chemical Research (RIKEN), Tokyo, Japan

S. Maeda
Laboratory for Diabetic Nephropathy, SNP Research Center, The Institute of Physical and Chemical Research (RIKEN), Tokyo, Japan

T. Takei · K. Ito · K. Honda · K. Uchida · K. Tsuchiya · K. Nitta · W. Yumura · H. Nihei
Department of Medicine, Kidney Center, Tokyo Women's Medical University, Tokyo, Japan

T. Ujiie
Department of Urology, Iwate Prefectural Ofunato Hospital, Iwate, Japan

Y. Nagane
Department of Urology, Sanai Hospital, Iwate, Japan

Y. Suzuki · T. Fujioka
Department of Urology, Iwate Medical University, Iwate, Japan

Y. Nakamura (✉)
Laboratory of Molecular Medicine, Human Genome Center, Institute of Medical Science, University of Tokyo, 4-6-1 Shirokanedai, Minato-ku, Tokyo 108-8639, Japan
Tel. +81-3-5449-5372; Fax +81-3-5449-5433
e-mail: yusuke@ims.u-tokyo.ac.jp

Introduction

Immunoglobulin A nephropathy (IgAN [MIM161950]), a disease characterized by predominant IgA deposits in glomerular mesangial areas, is the most common type of glomerulonephritis (GN); its prevalence may be as high as 50% of all cases of GN in Asia, especially among the Japanese. Long-term follow-up studies of biopsy-proven cases of IgAN have revealed that 20%–30% of patients progress to end-stage renal disease within 20 years of GN onset (Galla 1995; Floege and Feehally 2000).

The pathogenesis of IgAN is unknown, but accumulated data suggest that some genetic factors are involved in disease susceptibility (Galla 2001). The prevalence of IgAN seems to reflect demographic and ethnic characteristics of the populations studied; moreover, several cases of familial IgAN (Julian et al. 1985; Scolari et al. 1999) and higher risk of identical twins to IgAN (Tolkoff-Rubin et al. 1978; Sabatier et al. 1979) have been reported. Investigators have